Dornier et al., http://www.jcb.org/cgi/content/full/jcb.201201133/DC1

A

	Tspan5	Tspan17	Tspan14	Tsp26A	Tsp12	Tspan33	Tsp86D	Tsp3A	Tspan15	Tspan10	CD151
Tspan5	100	64	56	44	38	37	35	33	28	25	22
Tspan17			46	36	30	33	31	30	24	24	20
Tspan14				40	32	34	35	33	27	24	22
Tsp26A					36	28	30	31	25	22	23
Tsp12						27	28	30	21	22	19
Tspan33							37	35	28	25	21
Tsp86D								74	25	27	22
Tsp3A									25	25	21
Tspan15										19	19
Tspan10											18
CD151											100

B

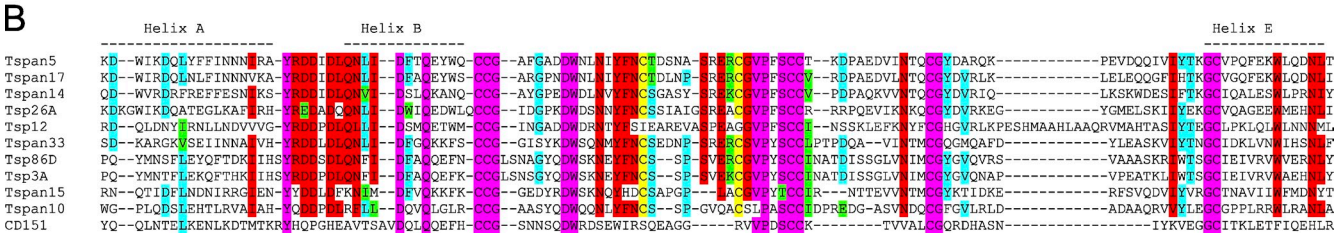

Figure S1. **An evolutionary conserved subfamily of tetraspanins.** (A) Amino acid identity levels between *H. sapiens* (Tspan5, 17, 14, 33, 15, 10), *D. melanogaster* (Tsp26A, 86D, 3A), and *C. elegans* (Tsp12) TspanC8 tetraspanins. The prototypal tetraspanin CD151 is also included for comparison. Human tetraspanins have most often less than 30% identity with each other. (B) Sequence alignment of the second extracellular domain of CD151 and the different *H. sapiens*, *D. melanogaster*, and *C. elegans* TspanC8 tetraspanins. This domain is highly divergent within the tetraspanin superfamily with the exception of a few residues that probably maintain the tetraspanin fold (pink). In contrast, TspanC8 tetraspanins share many conserved residues (red, >80% conservation; blue, >60% conservation; green, conservative substitutions) within this domain. The two additional cysteines that are the hallmark of TspanC8 are in yellow. Note that although Tsp12 has only six cysteines in the large extracellular domain, it shares many residues characteristic of TspanC8. The three conserved helices of this domain are shown on top of the sequences.

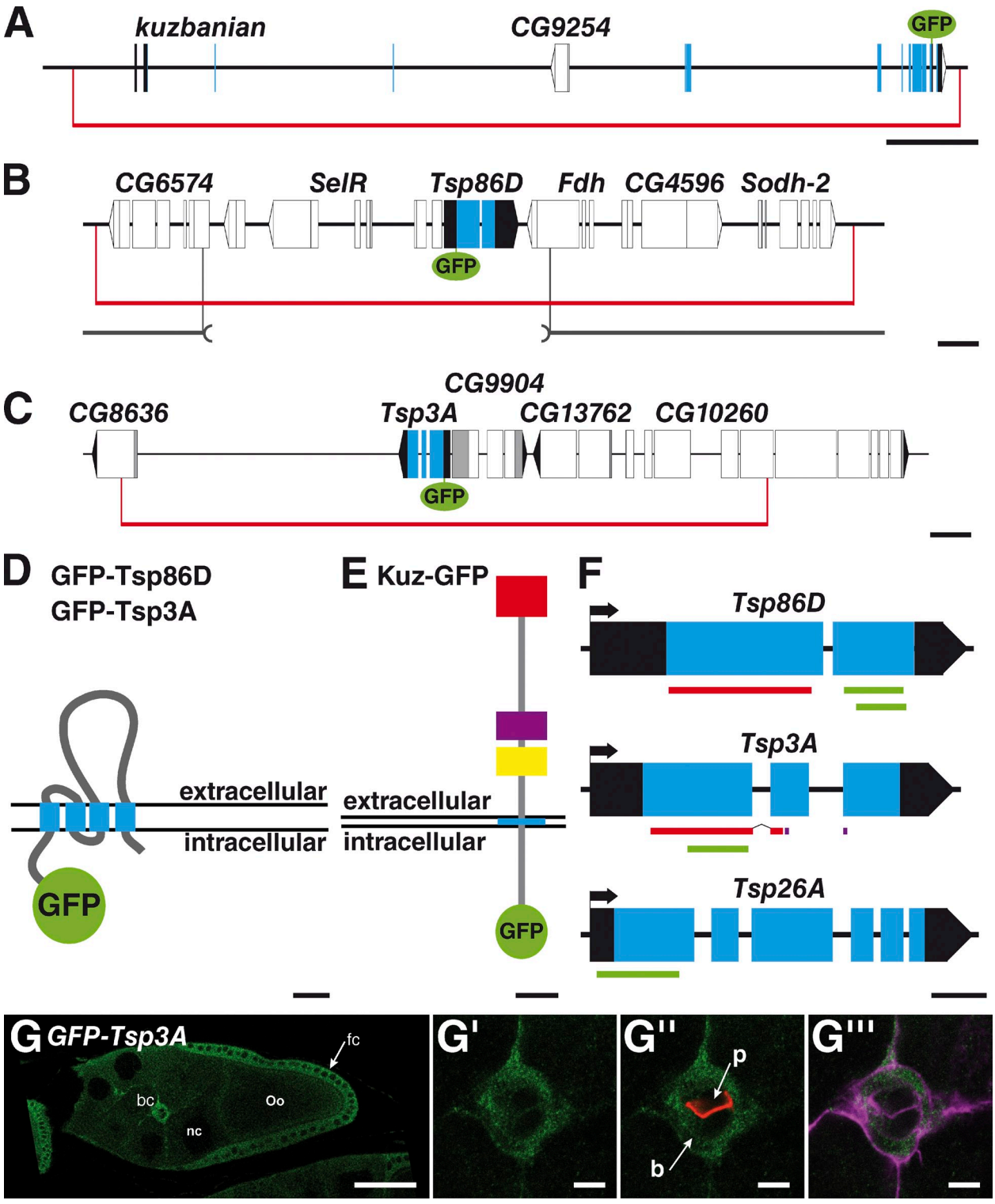

Figure S2. **Genetic tools.** (A–C) Schematic representation of the *kuz* (A), *Tsp86D* (B), and *Tsp3A* (C) genomic regions. The *kuz*, *Tsp86D*, and *Tsp3A* open reading frame (ORF) are in blue. 5′ and 3′ UTRs are in black. Exons from neighboring genes are in white. The BACs used in this study are indicated in red. GFP (green) was inserted at the 3′ and 5′ ends of *kuz* and *Tsp86D/Tsp3A* ORFs, respectively. The $Tsp86D^{\Delta 3}$ deficiency is indicated in gray. Bars: (A) 10 kb; (B and C) 1 kb. (D and E) Domain structure of GFP-Tsp86D/3A and Kuz-GFP (transmembrane segment, blue; prodomain of Kuz, red; metalloprotease domain, purple; disintegrin domain, yellow; GFP, green). Bars: (D) 20 aa; (E) 200 aa. (F) Sequence targeted by the dsRNAi and shmiR constructs used in this study (NIG-Fly, red; VDRC, green; shmiR, purple). The *Tsp86D*, *Tsp26A*, and *Tsp3A* transcripts are represented as in B. Bar, 200 nt. (G–G′′′) GFP-Tsp3A (anti-GFP, green; Fas3, red in G′′; actin, red in G′′′) was detected in migrating border cells (b) and in follicular cells. Polar cells (p) exhibited lower levels of GFP-Tsp3A. GFP-Tsp3A appears to be expressed similarly as GFP-Tsp86D and complementary to Kuz-GFP (see Fig. 6). Bars: (G) 40 µm; (G′and G′′) 5 µm.

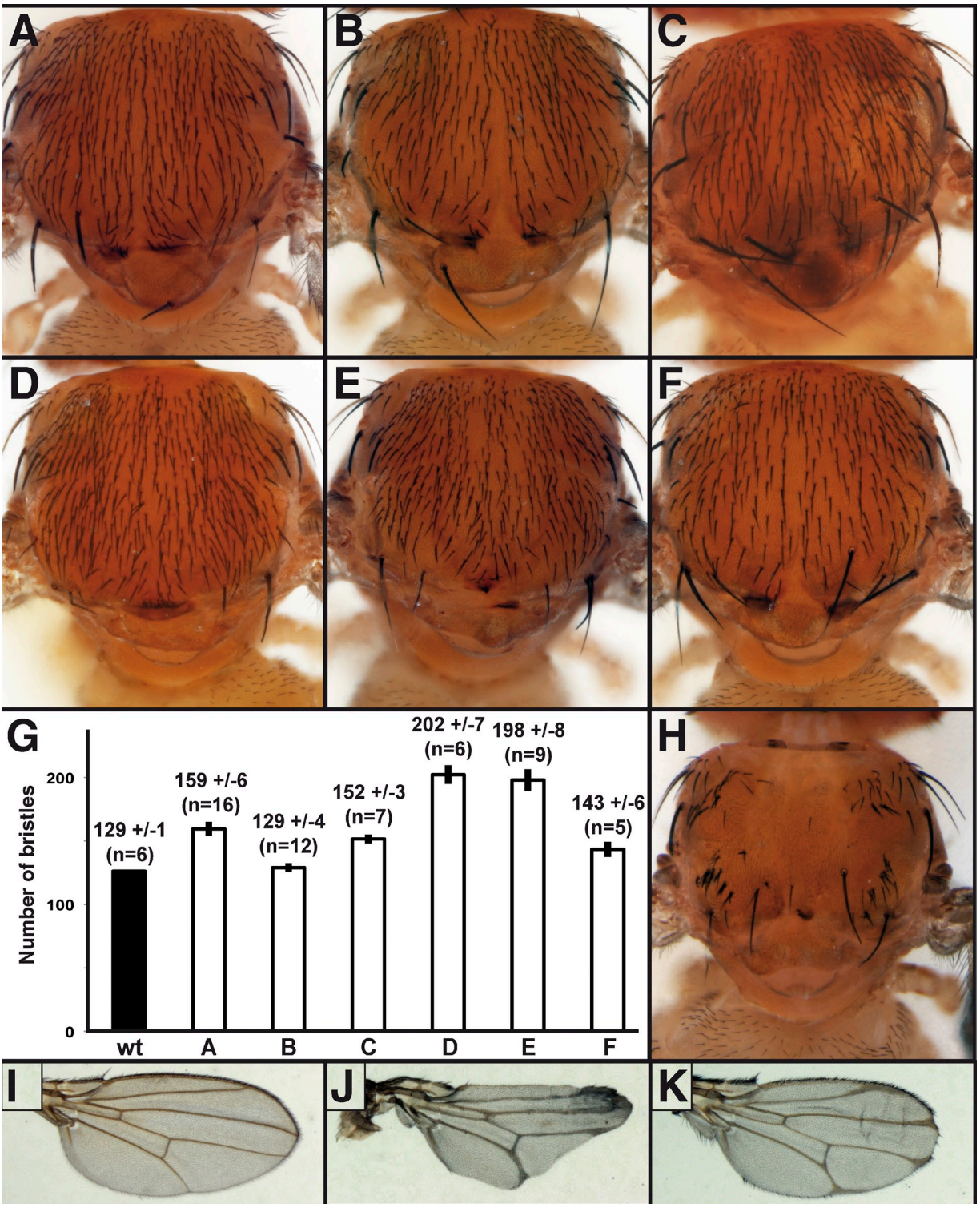

Figure S3. **Functional redundancy between *Drosophila Tsp86D, Tsp26A,* and *Tsp3A*.** (A–F) Pattern of sensory organs in adult flies silenced for *Tsp3A* (A), *Tsp26A* (B), *Tsp86D* (C), *Tsp3A* and *Tsp26A* (D), *Tsp3A* in a *Tsp86D* heterozygous background (E), and *Tsp26A* in a *Tsp86D* heterozygous background (F). Silencing was achieved using *ap*-GAL4. See Fig. 2 for a wild-type control and Table S1 for complete genotypes. (G) Histogram showing the number of bristles located in dorsal-central rows 1–5 of the notum (*n* is the number of scored flies for each genotype). The genotypes are indicated by letters corresponding to the other panels of this figure. For each genotype (except B), the distribution was significantly different from wild type (wt; χ^2 test, $P < 0.01$). (I–K) Wing margin and vein pattern in adult flies silenced for *kuz* (J) and *Tsp3A*, *Tsp26A*, and *Tsp86D* (K). Silencing was performed using *sd*-GAL4. A wild-type control is shown in I. Loss of TspanC8 activity in the wing results in wing nicks and vein-thickening *Notch*-like phenotypes that are milder than those seen upon the silencing of *kuz*.

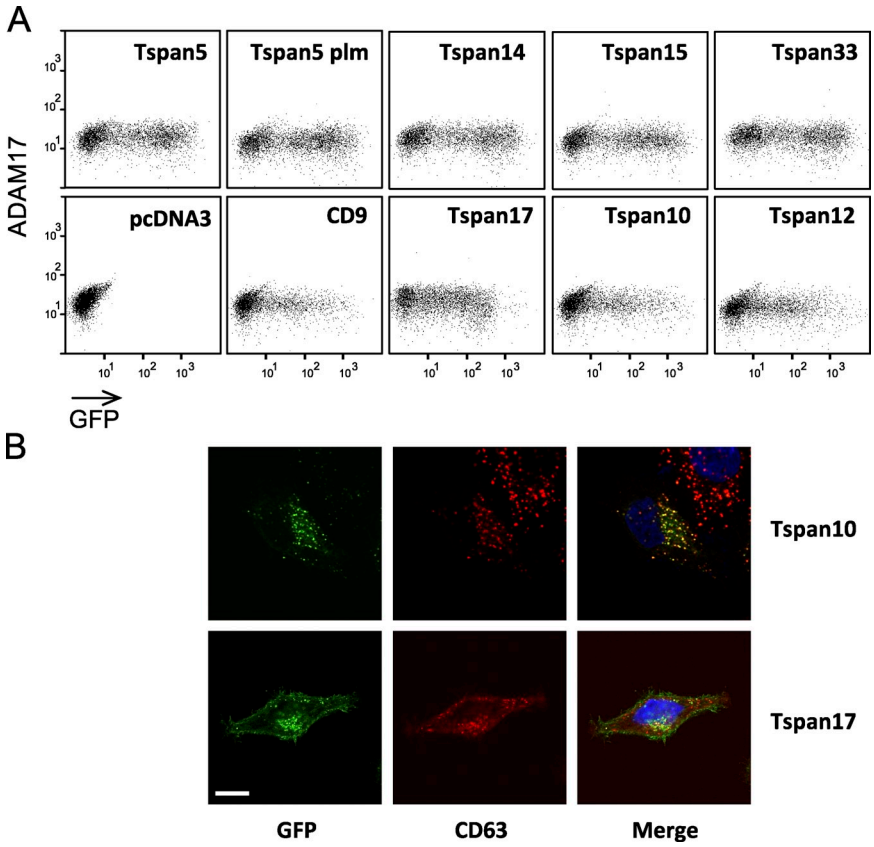

Figure S4. **Effect of TspanC8 tetraspanins on ADAM17 surface expression and codistribution of Tspan10 and Tspan17 with CD63.** (A) Flow cytometry analysis of the surface expression of ADAM17 in HeLa cells transiently transfected with different GFP-tagged tetraspanins. (B) Confocal microscopy analysis of GFP-tagged Tspan10 and Tspan17 (green) and CD63 (red) localization (red) in permeabilized HeLa cells. Bar, 10 µm. These experiments were performed at least twice.

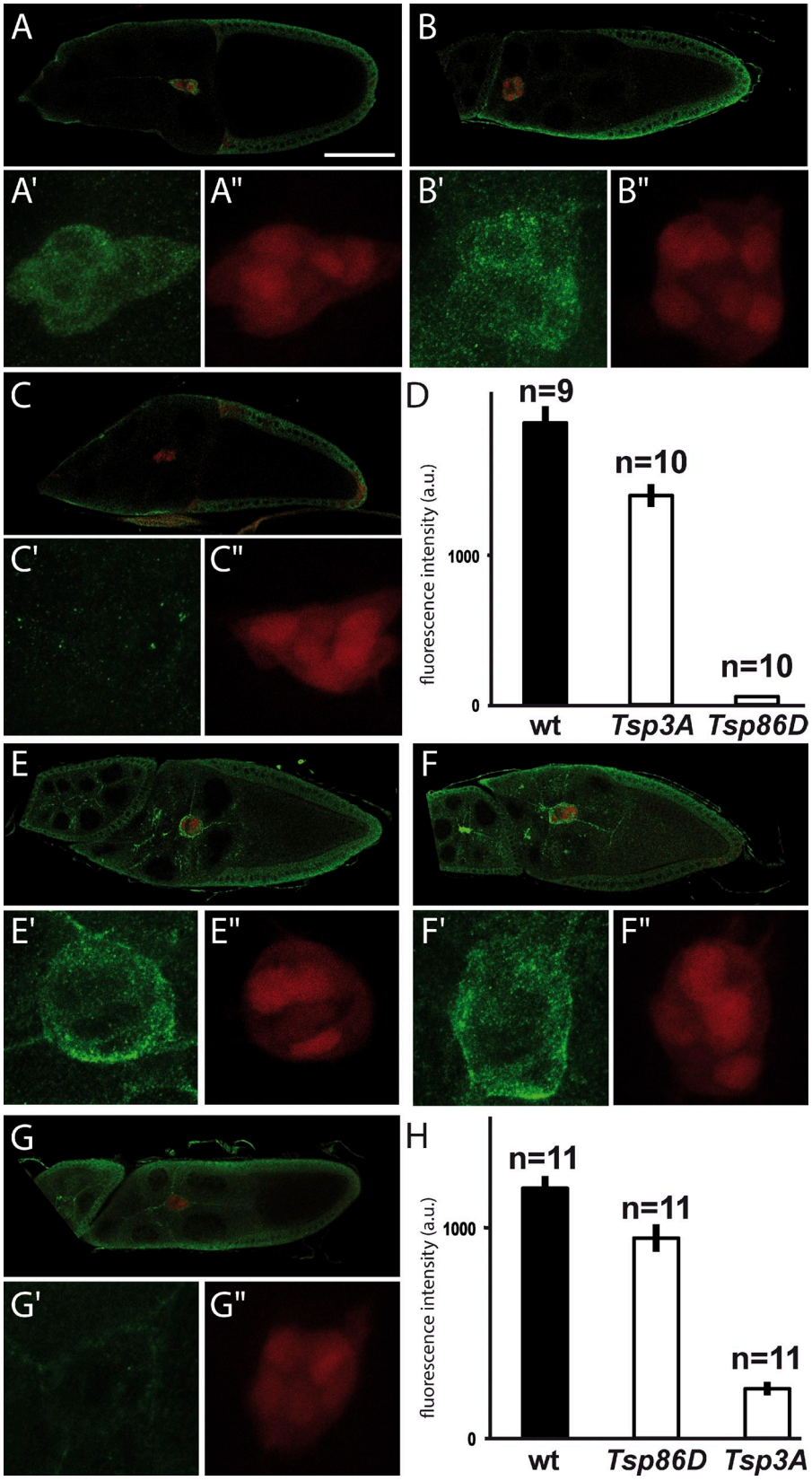

Figure S5. **Efficient and specific silencing of Tsp3A and Tsp86D in border cells.** (A–D) The expression of GFP-Tsp86D (green) was efficiently and specifically silenced in border cells (marked by the expression of RFP under the control of *slbo*-GAL4) by dsRNA directed against Tsp86D (C–C′′). In the absence of dsRNA (A–A′′) or in the presence of dsRNA directed against Tsp3A (B–B′′), GFP-Tsp86D was detected in border cells. The GFP fluorescence signal was measured to estimate the relative levels of GFP-Tsp86D (D; a.u.: arbitrary units). (E–G′′) Conversely, the expression of GFP-Tsp3A (green; no dsRNA in E–E′′) was efficiently silenced by dsRNA directed against Tsp3A (G–G′′) expressed but not by Tsp86D dsRNA (F–F′′). Unfortunately, the expression of GFP-Tsp3A and GFP-Tsp86D was too low in imaginal tissues to evaluate the efficiency of silencing in these tissues. (H) Quantification of the GFP-Tsp3A signal as in D.

Table S1. **Genotypes**

Figures	Genotypes
Fig. 2, A–C	w; ap-GAL4/+
Fig. 2, D–F	w; ap-GAL4/UAS-dsRNA *tsp3A*, UAS-dsRNA *tsp26A*; *Tsp86D*$^{[\Delta 3]}$/+
Fig. 2, G and H	(Tsp3A^{RNAi}): y w P[ry, hs-FLP]1.22 P[mw, ptub-GAL4] P[mw, UAS-GFP]/w; UAS-dsRNA *tsp3A*/+; P[neo, FRT]82B, P[mw, ptub-GAL80]/P[ry, neo, FRT]82B
Fig. 2 H	(Tsp26A^{RNAi}): y w P[ry, hs-FLP]1.22 P[mw, ptub-GAL4] P[mw, UAS-GFP]/w; UAS-dsRNA *tsp26A*/+; P[neo,FRT]82B, P[mw, ptub-GAL80]/P[ry, neo, FRT]82B
Fig. 2 H	(Tsp86D^{RNAi}): y w P[ry, hs-FLP]1.22 P[mw, ptub-GAL4] P[mw, UAS-GFP]/w; P[neo, FRT]40A, P[mw, ptub-GAL80]/P[ry, neo, FRT]40A; UAS-dsRNA *tsp86D*/+
Fig. 2 H	(Tsp86D$^{[\Delta 3]}$): y w P[ry, hs-FLP]1.22 P[mw, ptub-GAL4] P[mw, UAS-GFP]/w; ; P[neo, FRT]82B, P[mw, ptub-GAL80]/P[ry, neo, FRT]82B, *Tsp86D*$^{[\Delta 3]}$
Fig. 2 H	(wt): y w P[ry, hs-FLP]1.22 P[mw, ptub-GAL4] P[mw, UAS-GFP]/w; ; P[neo, FRT]82B, P[mw, ptub-GAL80]/P[ry, neo, FRT]82B
Fig. 7, B, C, and H	(wt): w, c306-Gal4/w; slbo-GAL4, UAS-GFP/+
Fig. 7, B, C, and H	(TspanC8): w, c306-Gal4/w; slbo-GAL4, UAS-GFP/UAS-dsRNA *tsp3A*, UAS-dsRNA *tsp26A* ; UAS-dsRNA *tsp86D*/+
Fig. 7, B and C	(kuz): w, c306-Gal4/w; slbo-GAL4, UAS-GFP/dsRNA *kuz*
Fig. 7, D–D′′′	w; M[3xP3-RFP.attP.w+.*kuz*^{GFP}]51C/M[3xP3-RFP.attP.w+ *kuz*^{GFP}]51C
Fig. 7, E–E′′′	w; PBac{y[+]-attP-3B. ^{GFP}*tsp86D*}VK00002/PBac{y[+]-attP-3B. ^{GFP}*tsp86D*}VK00002
Fig. 7, F–F′ and L	(wt): w; slbo-GAL4, M[3xP3-RFP.attP.w+.*kuz*^{GFP}]51C/+
Fig. 7, G–G′ and L	(TspanC8): w; slbo-GAL4, M[3xP3-RFP.attP.w+.*kuz*^{GFP}]51C/UAS-dsRNA *tsp3A*, UAS-dsRNA *tsp26A*; UAS-dsRNA *tsp86D*/+
Fig. 7, I–I′ and L	(wt): w; slbo-Gal4/+; M[3xP3-RFP, NRE-pGR]86Fb/+
Fig. 7, J–J′, K–K′, and L	(TspanC8): w; slbo-Gal4/UAS-dsRNA *tsp3A*, UAS-dsRNA *tsp26A*; M[3xP3-RFP, NRE-pGR]86Fb/UAS-dsRNA *tsp86D*
Fig. 7 L	(kuz): w; slbo-Gal4/UAS-dsRNA *kuz*; M[3xP3-RFP, NRE-pGR]86Fb/+
Fig. S2, G–G′′′	w/w; PBac{y[+]-attP-9A. ^{GFP}*tsp3A* }VK00019/PBac{y[+]-attP-9A. ^{GFP}*tsp3A* }VK00019
Fig. S3 A	w/w; ap-GAL4/+; UAS-dsRNA *tsp3A*/+
Fig. S3 B	w/w; ap-GAL4/+; UAS-dsRNA *tsp86D*/+
Fig. S3 C	w/w; ap-GAL4/UAS-dsRNA *tsp26A*
Fig. S3 D	w/w; ap-GAL4/UAS-dsRNA *tsp3A*, UAS-dsRNA *tsp26A*
Fig. S3 E	w/w; ap-GAL4/UAS-dsRNA *tsp3A*; tsp86D$^{[\Delta 3]}$/+
Fig. S3 F	w/w; ap-GAL4/UAS-dsRNA *tsp26A*; tsp86D$^{[\Delta 3]}$/+
Fig. S3 H; Fig. 2, I–I′′ and J–J′′	w/w; ap-GAL4/UAS-dsRNA *tsp3A*, UAS-dsRNA *tsp26A*; UAS-dsRNA *tsp86D*/+
Fig. S3 I	w, sd-GAL4/w
Fig. S3 J	w, sd-GAL4/w; UAS-dsRNA *tsp3A*, UAS-dsRNA *tsp26A*/+; UAS-dsRNA *tsp86D*/+
Fig. S3 K	w, sd-GAL4/w; UAS-dsRNA *kuz*
Fig. S5, A–A′′ and D	(wt): w/w; slbo-Gal4, UAS-nlsRFP/PBac{y[+]-attP-3B. ^{GFP}*tsp86D*}VK00002
Fig. S5, B–B′′ and D	(Tsp3A): w/w; slbo-Gal4, UAS-nlsRFP/PBac{y[+]-attP-3B. ^{GFP}*tsp86D*}VK00002; UAS-dsRNA *tsp3A*/+
Fig. S5, C–C′′ and D	(Tsp86D): w/w; slbo-Gal4, UAS-nlsRFP/PBac{y[+]-attP-3B. ^{GFP}*tsp86D*}VK00002; UAS-dsRNA *tsp86D*/+
Fig. S5, E–E′ and H	(wt): w/w; slbo-Gal4, UAS-nlsRFP/CyO; PBac{y[+]-attP-9A. ^{GFP}*tsp3A* }VK00019/+
Fig. S5, F–F′′ and H	(Tsp86D): w/w; slbo-Gal4, UAS-nlsRFP/UAS-dsRNA *tsp86D*/+; PBac{y[+]-attP-9A. ^{GFP}*tsp3A* }VK00019/+
Fig. S5, G–G′′ and H	(Tsp3A): w/w; slbo-Gal4, UAS-nlsRFP/UAS-dsRNA *tsp3A*/+; PBac{y[+]-attP-9A. ^{GFP}*tsp3A* }VK00019/+